Conjugate heat transfer to a laminar confined impinging planar jet

O. Manca,[a] V. Naso,[b] G. Ruocco[b]
[a]*Dipartimento di Ingegneria Aerospaziale, Seconda Università degli studi di Napoli, Via Roma 29, 81031 Aversa, Italy*
[b]*DETEC, Università degli studi di Napoli Federico II, Piazzale Tecchio 80, 80125 Napoli, Italy*

Abstract

A numerical analysis for fluid flow and conjugate convection/conduction heat transfer of a single confined air laminar slot jet on a discretely heated finite thickness plate has been performed. A highly non uniform grid has been set up for the resolution of the boundary layer. Streamlines and isotherms patterns at different heat source lengths and jet Reynolds numbers are presented. The local Nusselt number is nearly independent of the impinged plate thickness whereas it is affected by the heater length.

1 Introduction

In recent years jet impingement heat transfer has been widely used as a high-performance technique for heating, cooling or drying a surface, since it is able to supply high heat transfer rates to the target surface. This technique is attractive for the removal of very high power densities encountered in a variety of environments and engineering applications, such as the processing of metals and glass, as well as electronics equipment cooling. Therefore, interest in both experimental and numerical assessment continues nowadays, for a variety of device configurations and jet arrangements, as reported by Martin[1] and, more recently, by Viskanta[2] and Webb & Ma[3].

A common configuration is the injection of the cooling fluid into a confined space, normal to the heated surface. A great deal of work has been performed on this phenomenology and relative to the laminar regime, e.g. the recent work by Chou & Hung[4], among others. It is clear from their work that an important, yet critical aspect of the modeling of an impinging jet, has still to be met, with

reference to the thermal boundary condition which must be assigned to the target surface.

In preliminary analyses, a uniform value of either temperature or thermal flux was applied to the surface. A different approach may be used, which takes into account the effective temperature distribution in the solid region; thus, the assignment of a proper thermal boundary condition has been transferred to the rear surface of the target solid. Several workers have carried out studies on this line. Wang et al.[5] proposed, for a liquid free jet in an axisymmetrical configuration, to match at the solid-fluid interface the analytical solutions which were separately derived for the two phases. Faghri et al.[6] reported the comparison between experimental and numerical results for a similar configuration. Alkam & Butler[7] investigated the unsteady case, for a variety of solid-fluid combinations.

Two papers dealed with the microcircuitry cooling, both relative to a liquid free jet configuration. Zumbrunnen et al.[8] presented some comparisons between experimental and numerical results, the latter being determined by surface temperature distributions derived from measurements. Wang et al.[9] used the analytical method published by the same workers[5].

Schafer et al.[10] studied a laminar slot jet to cool an array of discrete heat sources, which were flush-mounted in a channel. However, the study of the conjugate effects was limited to the sources geometry.

The present paper addresses the unanswered question of how the conduction in a discretely heated finite thickness plate influences the convection heat transfer to a laminar, submerged and confined impinging jet. Emphasis is given to the effects of the geometrical characteristics of the solid substrate on the convective heat transfer. A special, yet simple, solution strategy is adopted to resolve the boundary layer and ensure convergence.

2 Analysis

In this study a single nozzle configuration is simulated; thus the jet is supposed to discharge from a slot duct to the confined space with a uniform velocity profile. The following assumptions are adopted: the flow is laminar, two-dimensional, steady and incompressible with temperature-dependent properties; the viscous heat dissipation and the buoyancy forces are neglected. A region of the impinged surface rear is at a prescribed uniform temperature, t_p; the rest of this surface and the upper confining plate are adiabatic. No-slip conditions are applied to both confining surfaces. The outer boudaries of the system are considered adiabatic; at the outflow boundary, the momentum conservation equations are rendered locally parabolic, as the corresponding streamwise diffusion is assumed to be zero. Due to the simmetry about the midplane, only a half section of the domain is depicted in fig.1.

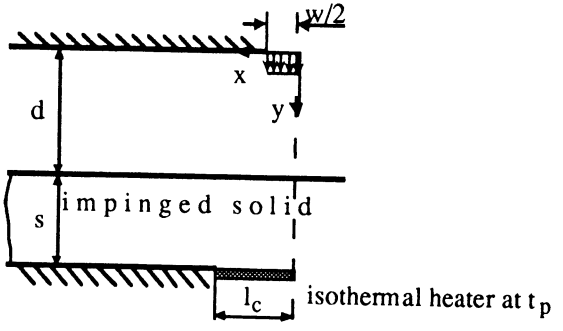

Figure 1: The investigated fluid and solid domains

With reference to Cartesian coordinates, the governing equations in conservative form may be written as follows:

$$\frac{\partial(\rho' U)}{\partial X} + \frac{\partial(\rho' V)}{\partial Y} = 0 \tag{1}$$

$$\frac{\partial(\rho' U^2)}{\partial X} + \frac{\partial(\rho' UV)}{\partial Y} = \frac{1}{Re_j}\frac{\partial}{\partial X}\left(\mu'\frac{\partial U}{\partial X}\right) + \frac{1}{Re_j}\frac{\partial}{\partial Y}\left(\mu'\frac{\partial U}{\partial Y}\right) - \frac{\partial P}{\partial X} \tag{2}$$

$$\frac{\partial(\rho' UV)}{\partial X} + \frac{\partial(\rho' V^2)}{\partial Y} = \frac{1}{Re_j}\frac{\partial}{\partial X}\left(\mu'\frac{\partial V}{\partial X}\right) + \frac{1}{Re_j}\frac{\partial}{\partial Y}\left(\mu'\frac{\partial V}{\partial Y}\right) - \frac{\partial P}{\partial Y} \tag{3}$$

$$\frac{\partial(\rho' UT)}{\partial X} + \frac{\partial(\rho' VT)}{\partial Y} = \frac{1}{Re_j Pr}\left[\frac{\partial}{\partial X}\left(\frac{k_f'}{c_p'}\frac{\partial T}{\partial X}\right) + \frac{\partial}{\partial Y}\left(\frac{k_f'}{c_p'}\frac{\partial T}{\partial Y}\right)\right] \tag{4}$$

$$\frac{\partial}{\partial X}\left(k_s'\frac{\partial T}{\partial X}\right) + \frac{\partial}{\partial Y}\left(k_s'\frac{\partial T}{\partial Y}\right) = 0 \tag{5}$$

The following driving non-dimensional quantities are defined:

$$X = \frac{x}{w};\quad Y = \frac{y}{w};\quad D = \frac{d}{w};\quad L_c = \frac{l_c}{w};\quad S = \frac{s}{w};\quad U = \frac{u}{v_j};\quad V = \frac{v}{v_j};$$

$$T = \frac{t - t_j}{t_p - t_j};\quad P = \frac{p - p_\infty}{\rho_j v_j^2};\quad Re_j = \frac{\rho_j v_j w}{\mu_j} \tag{6}$$

The dimensionless fluid and solid properties may be defined as:

$$k_f' = \frac{k_f}{k_j};\ k_s' = \frac{k_s}{k_\infty};\ \rho' = \frac{\rho}{\rho_j};\ c_p' = \frac{c_p}{c_{pj}};\ \mu' = \frac{\mu}{\mu_j};\ Pr = \frac{c_{pj}\,\mu_j}{k_j};\ K = \frac{k_f}{k_s} \tag{7}$$

For the sake of simplicity, in the following the primes are dropped out.

The pertaining boundary conditions, relative to the various domain frontiers, are defined as follows:

Jet inlet:

$$(0 \le X \le 0.5;\ Y = 0)\text{: } U = 0,\ V = 1.5\,(1 - 4\,X^2),\ T = 0 \tag{8}$$

Fluid symmetry plane:

$$(X = 0;\ 0 < Y < D)\text{: } U = 0,\ \frac{\partial V}{\partial X} = 0,\ \frac{\partial T}{\partial X} = 0 \tag{9}$$

Solid symmetry plane:

$$(X = 0;\ D \le Y \le D + S)\text{: } \frac{\partial T}{\partial X} = 0 \tag{10}$$

Solid–fluid interface:

$$(0 \le X < \infty;\ Y = D)\text{: } U = 0,\ V = 0,\ T_f = T_s,\ K\frac{\partial T_f}{\partial Y} = \frac{\partial T_s}{\partial Y} \tag{11}$$

Impingement plate rear, heated zone:

$$(0 \le X \le L_c;\ Y = D + S)\text{: } T = 1 \tag{12}$$

Impingement plate rear, adiabatic zone:

$$(L_c < X < \infty;\ Y = D + S)\text{: } \frac{\partial T_s}{\partial Y} = 0 \tag{13}$$

Solid at undisturbed distance:

$$(X \to \infty;\ D \le Y \le D + S)\text{: } \frac{\partial T_s}{\partial X} = 0 \tag{14}$$

Fluid outlet:

$$(X \to \infty;\ 0 < Y < D)\text{: } V = 0,\ \frac{\partial U}{\partial X} = 0,\ \frac{\partial T_f}{\partial X} = 0 \tag{15}$$

Confinement plate:

$$(1 \le X < \infty;\ Y = 0)\text{: } U = 0,\ V = 0,\ \frac{\partial T_f}{\partial X} = 0 \tag{16}$$

3 Numerical procedure and solution

The problem has been solved using the well-known Patankar's finite-volume, semi-implicit iterative procedure[11]. Indeed, the final discretization equation can be written as:

$$a_P \phi_P = a_N \phi_N + a_E \phi_E + a_S \phi_S + a_W \phi_W + S^{\phi} \tag{17}$$

where ϕ is the scalar quantity (U, V, P, T), W, N, E, S are the locations of the grid nodes and S^{ϕ} is the appropriate discretized source term. As the "a" coefficients depend upon the various scalar quantities ϕ themselves, the resulting system is nonlinear and interlinked. A line Gauss-Seidel solver has been used, and the enhancements proposed by Van Doormaal & Raithby[12] concerning the overrelaxation and convergence criteria have been applied to the present study.

A great deal of care has been used to generate the results by using a highly nonuniform grid. In order to resolve the extremely thin boundary layer on the surface due to the impingement and redirection of flow, the grid lines adjacent to the plate and to the jet midplane must be very closely spaced. An algebraic mesh generation procedure was designed, which featured several stretching parameters in order to yield the grid thickening about the jet midplane and the confining surfaces. The final grid was chosen by an iterative approach which gradually increased the stretching parameters: at each iteration step the new solution was found exploiting the previous one as the starting condition. The grid refinement was carried on until the local Nusselt number, as defined in the following, exhibited an invariant behaviour, i.e. in the worst case the maximum relative deviation between the values calculated with two successive grids was less than 10^{-3}. The grid size of 50 and 60 lines, respectively in the X and Y directions, was chosen for all computations in the following, together with 10 additional lines in the solid.

As far as the effect of the target surface length on the computational accuracy is concerned, a preliminary study showed that, compared with local Nusselt numbers for the case with L_∞=40, the maximum deviations of the local Nusselt numbers for the case L_∞=20 were less than 0.3 %. Therefore, in order to take suitably into account the conductive heat diffusion in the plate, an undisturbed lenght L_∞=20 was chosen.

Equations (1-3) have been first solved in the fluid domain and then eqns (4) and (5) have been solved in both fluid and solid domains; a harmonic mean has been used at the fluid-solid interface to deal with the discontinuities in the thermal conductivities. Convergence of the numerical results was assumed when the maximum absolute difference between two consecutive iterations was within 10^{-6} for U and V, 10^{-8} for P and 10^{-4} for T; the global mass conservation

between the inlet and outlet sections of the fluid was verified at less than 10^{-3}, whereas the local mass unbalance in each finite volume was no greater than 10^{-6}.

Once the thermal field is obtained, the local Nusselt number can be evaluated as

$$Nu_x = \frac{h_x\, w}{k_f} = \frac{\partial T}{\partial Y}\Bigg|_{Y=D} \tag{18}$$

4 Results and discussion

In the present study reference is made to an aluminum impinged plate by an air laminar jet. The values of the explored parameters are: D=4, S=0.2-1.0, L_c=1-10, L_∞=10 and L_∞=20, Pr=0.7, Re_j=200 and Re_j=800.

The streamlines and isotherms patterns are presented in figs.2, with D=4, S=1, L_c=1, L_∞=20, Pr=0.7 and Re_j=200. In fig.2a we can observe a recirculation cell near the impinged plate, approximately at 13 diameters from the jet midplane. It can be looked at as the origin of a hydraulic jump typical of non submerged liquid impinging jets. This is likely due to the low value of Reynolds number, which determines an incompressible flow very similar to that of a liquid. In the region closer to the jet another recirculation cell dominates the fluid dynamic field confined by the jet and by the two solid surfaces. This cell has already been noticed by many authors, such as Polat et al.[13]. Finally, in agreement with the results reported in the literature, there is a weaker recirculation zone in the proximity of the jet, adjacent to the confining plate, which is determined by the depression caused by the jet itself. Figure 2b shows that at about X=4 the fluid temperature becomes higher than the solid temperature; therefore, beyond X>4 up to nearly X=8 heat is transferred from the fluid to the impinged plate.

The streamlines and isotherms patterns are presented in figs.3, with D=4, S=1, L_c=1, L_∞=20, Pr=0.7 and Re_j=800. Figure 3a shows the displacement of the main recirculation cells toward the outlet section of the domain and the widening of the cell near the confining upper surface at the greater Reynolds number. As exhibited by fig.3b, the heat transfer rate from the fluid to the wall is greater at the higher Reynolds number, where the hotter fluid region is thinner in the Y direction but somewhat thicker in the X direction.

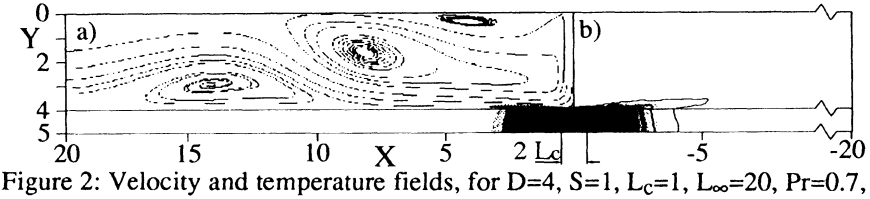

Figure 2: Velocity and temperature fields, for D=4, S=1, L_c=1, L_∞=20, Pr=0.7, Re_j=200: a) streamlines, b) isotherms.

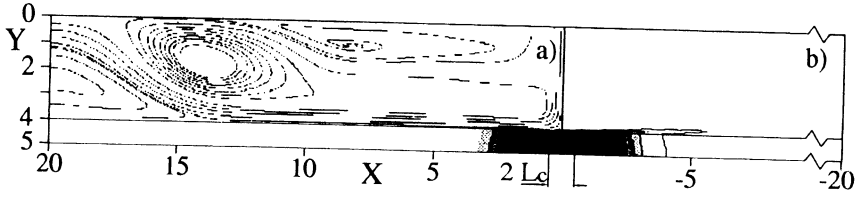

Figure 3: Velocity and temperature fields, for D=4, S=1, L_c=1, L_∞=20, Pr=0.7, Re_j=800: a) streamlines, b) isotherms.

The effect of the component width is pointed out by comparing figs.2 to figs.4, where streamlines and isotherms patterns with D=4, S=1, L_c=10, L_∞=20, Pr=0.7, Re_j=200 are reported. Comparing fig.2a to fig.4a one can notice nearly equal streamline patterns whereas the comparison of fig.2b to fig.4b shows marked differences in temperature profiles. As expected, the regions where the jet temperature remains low are smaller when the component is wider. Furthermore, it is evident that the recirculation cell near the impinged plate worsens the local heat transfer removal in the later case.

The values of local Nusselt number have been calculated by means of the proposed numerical procedure. The group $Nu_x/Re^{0.5}$ as a function of the X coordinate, for D=4, S=0 (isothermal plate), Pr=0.7, Re_j=200, L_∞=10, is first reported in fig.5. For the sake of comparison, the values presented in the numerical study carried out by Chou & Hung[4], for a purely fluid configuration, all parameters being the same, are presented in the same figure. A nearly 7% deviation between our local Nusselt number predicted values and those predicted by Chou & Hung can be noticed in the stagnation region. Greater deviations are pointed out in the jet outlet domain (X>5).This is likely due to the presence, in the present study, of the above mentioned main recirculation cells which worsen the heat transfer effectiveness.

The effect of impinged plate thickness and heater length on the local Nusselt number is pointed out in fig.6, where the term $Nu_x/Re^{0.5}$ as a function of the X coordinate, for D=4, Pr=0.7, Re_j=200, L_∞=20 and various L_c and S values, is plotted. First of all, it is noticed that in every case the local Nusselt number is unaffected by the plate thickness. Figure 6 also shows that, in the stagnation region, up to L_c=2 the wider the heater, the greater the local coefficient of heat

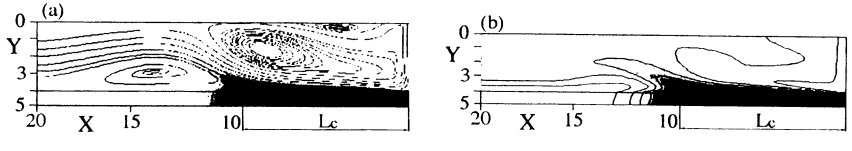

Figure 4: Velocity and temperature fields, for D=4, S=1, L_c=10, L_∞=20, Pr=0.7, Re_j=200: a) streamlines; b) isotherms.

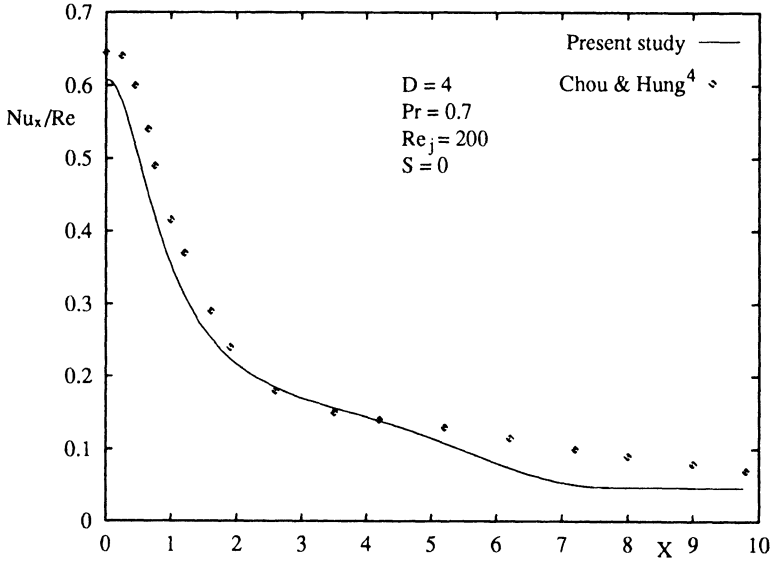

Figure 5: $Nu_x/Re^{0.5}$ vs X, for D=4, S=0, Pr=0.7, Re_j=200, L_∞=10.

removal, whereas only little deviations between values at L_c=2 and L_c=10 are exhibited in the X=0-1 range. Negative Nusselt numbers for $L_c \leq 2$ indicate that heat is transferred from the air to the plate in the X domain where the heat

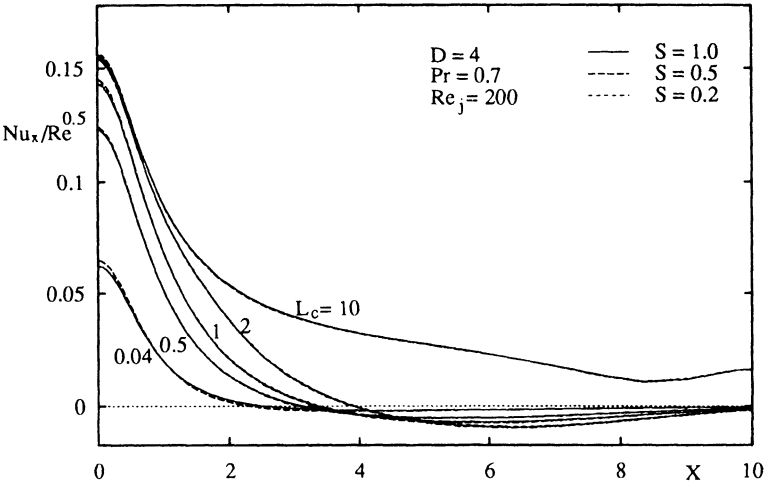

Figure 6: $Nu_x/Re^{0.5}$ vs X, for D=4, S=0.2-0.50-1.0, L_c=0.04-0.5-1-2-10, L_∞=20, Pr=0.7, Re_j=200.

diffusion in the solid is negligible, as already remarked observing thermal fields. At the maximum heater length (L_c=10) fluid temperatures are everywhere greater than those exhibited by the plate surface; the minimum attained by the Nusselt number at X≈8.5 denotes a reduced heat transfer rate caused by one of the two main recirculation cells.

5 Conclusions

The numerical analysis of conjugate heat transfer to a laminar confined impinging planar jet has shown the existence of recirculation cells between the confining plates.

The streamlines patterns in the conjugate problem are similar to those typical of the uncoupled problem. In the explored field of the process parameters the plate thickness does not affect the heat removal effectiveness. The impinged plate contributes to the heat removal when the heater width is less wide than four times the jet slot width.

6 Nomenclature

c_p constant pressure specific heat
d, D dimensional and dimensionless confinement plate-impinged solid distance
h_x local heat transfer coefficient
k thermal conductivity
K thermal conductivity ratio
l_c, L_c dimensional and dimensionless component half-width
L_∞ dimensionless undisturbed distance
Nu_x local Nusselt number
p, P dimensional and dimensionless pressure
Pr Prandtl number
Re Reynolds number
s, S dimensional and dimensionless impinged plate thickness
t, T dimensional and dimensionless temperature
u, U dimensional and dimensionless velocity component in the x direction
v, V dimensional and dimensionless velocity component in the y direction
w jet slot width
x, X dimensional and dimensionless coordinate parallel to the impinged solid
y, Y dimensional and dimensionless coordinate normal to the impinged solid

Greek symbols
μ dynamic viscosity
ρ density

Subscripts
f fluid
j fluid at jet inlet
p prescribed
s solid

Superscripts
' dimensionless

Acknowledgement

This work was funded by CNR with the grant 94.01887

References

1. Martin, H. Heat and Mass Transfer between Impinging Gas Jets and Solid Surfaces, *Advances in heat transfer*, ed J.P. Hartnett & T.F. Irvine Jr., Vol.13, pp 1-60, Academic Press, New York, 1977.
2. Viskanta, R. Heat Transfer to Impinging Isothermal Gas and Flame Jets, *Experimental Thermal Fluid Sci.*, 1993, **6**, 111-134.
3. Webb, B.W. & Ma, C.F. Single-phase liquid jet impingement heat transfer, *Advances in heat transfer*, ed J.P. Hartnett & T.F. Irvine Jr., Vol.26, pp 105-217, Academic Press, New York, 1995.
4. Chou, Y.J. & Hung, Y.H., Fluid flow and heat transfer of an extended slot jet impingement, *J. Thermophysics Heat Transfer*, 1994, **8**, 3, 538-545.
5. Wang, X.S., Dagan, Z. & Jiji, L.M., Conjugate heat transfer between a laminar impinging liquid jet and a solid disk, *Int. J. Heat Mass Transfer*, 1989, **32**, 11, 2189-2197.
6. Faghri, A., Thomas, S. & Rahman, M.M., Conjugate heat transfer from a heated disk to a thin liquid film formed by a controlled impinging jet, *J. Heat Transfer*, 1993, **115**, 116-123.
7. Alkam, M.K. & Butler, P.B., Transient conjugate heat transfer between a laminar stagnation zone and a solid disk, *J. Thermophysical Heat Transfer*, 1994, **8**, 4, 664-669.
8. Zumbrunnen, D.A., Incropera, F.P. & Viskanta, R., Convective heat transfer distributions on a plate cooled by planar water jets, *J. Heat Transfer*, 1989, **11**, 889-896.
9. Wang, X.S., Dagan, Z. & Jiji, L.M., Prediction of surface temperature and heat flux of a microelectronic chip with jet impingement cooling, *J. Electronic Packaging*, 1990, **112**, 57-62.
10. Schafer, D.M., Ramadhyani, S. & Incropera, F.P., Numerical simulation of laminar convection heat transfer from an in-line array of discrete sources to a confined rectangular jet, *Numer. Heat Transfer, Part A*, 1992, **22**, 121-141.
11. Patankar, S.V., *Numerical Heat Transfer and Fluid Flow*, Hemisphere Publishing Co., New York, 1980.
12. Van Doormaal, J.P. & Raithby, G.D., Enhancement of the SIMPLE method for predicting incompressible fluid flow, *Num. Heat Transfer*, 1984, **7**, 147-163.
13. Polat, S., Huang B., Mujumdar, A.S. & Douglas, W.J.M., Numerical flow and heat transfer under impinging jets: a review, Chapter 4, *Annual review of numerical fluid mechanics and heat transfer*, ed C.L. Tien & T.C. Chawla, pp 157-197, New York, 1989.